

GRAVITATIONAL-WAVE ASTRONOMY WITH INSPIRAL SIGNALS OF SPINNING COMPACT-OBJECT BINARIES

M. V. VAN DER SLUYS,¹ C. RÖVER,^{2,3} A. STROEER,^{1,4} V. RAYMOND,¹ I. MANDEL,¹ N. CHRISTENSEN,⁵ V. KALOGERA,¹
R. MEYER,² AND A. VECCHIO^{1,4}

Received 2007 October 8; accepted 2008 October 6; published 2008 October 23

ABSTRACT

Inspirals signals from binary compact objects (black holes and neutron stars) are primary targets of the ongoing searches by ground-based gravitational-wave interferometers (LIGO, Virgo, and GEO-600). We present parameter-estimation simulations for inspirals of black hole–neutron star binaries using Markov Chain Monte Carlo methods. For the first time, we both estimated the parameters of a binary inspiral source with a spinning, precessing component and determined the accuracy of the parameter estimation, for simulated observations with ground-based gravitational-wave detectors. We demonstrate that we can obtain the distance, sky position, and binary orientation at a higher accuracy than previously suggested in the literature. For an observation of an inspiral with sufficient spin and two or three detectors we find an accuracy in the determination of the sky position of the order of tens of square degrees.

Subject headings: binaries: close — gamma rays: bursts — gravitational waves — relativity

1. INTRODUCTION

Binary systems with compact objects—neutron stars (NS) and black holes (BH)—in the mass range $\sim 1\text{--}100 M_{\odot}$ are among the most likely sources of gravitational waves (GWs) for ground-based laser interferometers currently in operation (Cutler & Thorne 2002): LIGO (Barish & Weiss 1999), Virgo (Acernese et al. 2004), and GEO-600 (Willke et al. 2004). Merger-rate estimates are quite uncertain and for BH-NS binaries current detection-rate estimates reach from 0.0003 to 0.1 yr^{-1} for first-generation instruments (e.g., O’Shaughnessy et al. 2008). Upgrades to Enhanced LIGO/Virgo (2008–2009) and Advanced LIGO/Virgo (2011–2014) are expected to increase detection rates by factors of about ~ 8 and 10^3 , respectively.

The measurement of astrophysical source properties holds major promise for improving our physical understanding and requires reliable methods for parameter estimation. This is a challenging problem because of the large number of parameters (>10) and the presence of strong correlations among them, leading to a highly structured parameter space. In the case of high mass ratio binaries (e.g., BH-NS), these issues are amplified for significant spin magnitudes and large spin misalignments (Apostolatos et al. 1994; Grandclément et al. 2003; Buonanno et al. 2003). However, the presence of spins benefits parameter estimation through the signal modulations, although still presenting us with a considerable computational challenge. This was highlighted in the context of *LISA* observations (see Vecchio 2004; Lang & Hughes 2006) but no study has been devoted so far to ground-based observations.

In this Letter we examine for the first time the potential for parameter estimation of spinning binary inspirals with ground-based interferometers, including 12 physical parameters. Earlier studies (e.g., Jaranowski & Krolak 1994; Cutler & Flanagan 1994;

Poisson & Will 1995; Van den Broeck & Sengupta 2007) computed the potential accuracy of parameter estimation (e.g., using the Fisher matrix), but without performing a parameter estimation in practice (see the end of § 3 for a discussion). Also, Röver et al. (2006, 2007) explored parameter estimation for nonspinning binaries. We focus on BH-NS binaries where spin effects are strongest (Apostolatos et al. 1994), while at the same time we are justified to ignore the NS spin. We employ a newly developed Markov Chain Monte Carlo (MCMC) algorithm (Van der Sluys et al. 2008) applied on spinning inspiral signals injected into synthetic noise and we derive posterior probability-density functions (PDFs) of all 12 signal parameters. We show that although sky position is degenerate when using two detectors, we can still determine the mass and spin parameters to reasonable accuracy. With three detectors, the sky position and binary orientation can be fully resolved. We show that our accuracies are good enough to associate an inspiral event with an electromagnetic detection, such as a short gamma-ray burst (e.g., Nakar 2007).

2. SIGNAL AND OBSERVABLES

In this Letter we concentrate on the signal produced during the inspiral phase of two compact objects of masses $M_{1,2}$ in circular orbit. We focus on a fiducial BH-NS binary system with $M_1 = 10 M_{\odot}$ and $M_2 = 1.4 M_{\odot}$, so that we can ignore the NS spin. The BH spin S couples to the orbital angular momentum, leading to amplitude and phase modulation of the observed radiation due to the precession of the orbital plane during the observation. Here we model GWs by post-Newtonian (pN) waveforms at $^{1.5}$ -pN order in phase and Newtonian amplitude. We adopt the *simple-precession* limit (eqs. [51], [52], [59], and [63] in Apostolatos et al. 1994), appropriate for the single-spin system considered here. For simplicity (to speed up the waveform calculation), we ignore the *Thomas precession* (Apostolatos et al. 1994). In this approximation, the orbital angular momentum L and spin S precess with the *same* angular frequency around a fixed direction $\hat{J}_0 \approx \hat{J}$, where $\mathbf{J} = \mathbf{L} + \mathbf{S}$. During the inspiral phase the spin misalignment $\theta_{SL} \equiv \arccos(\hat{S} \cdot \hat{L})$ and $S = |\mathbf{S}|$ are constant. These approximated waveforms retain (at the leading order) all the salient qualitative features introduced by the spins, while allowing us to compute the waveforms analytically, at great speed. While this approach is justified for exploration of GW astronomy and development of parameter-estimation al-

¹ Department of Physics and Astronomy, Northwestern University, 2131 Tech Drive, Evanston, IL 60208.

² Department of Statistics, University of Auckland, Private Bag 92019, Auckland 1142, New Zealand.

³ Max-Planck-Institut für Gravitationsphysik, Callinstraße 38, 30167 Hannover, Germany.

⁴ School of Physics and Astronomy, University of Birmingham, Edgbaston, Birmingham B15 2TT, UK.

⁵ Physics and Astronomy Department, Carleton College, One North College Street, Northfield, MN 55057.

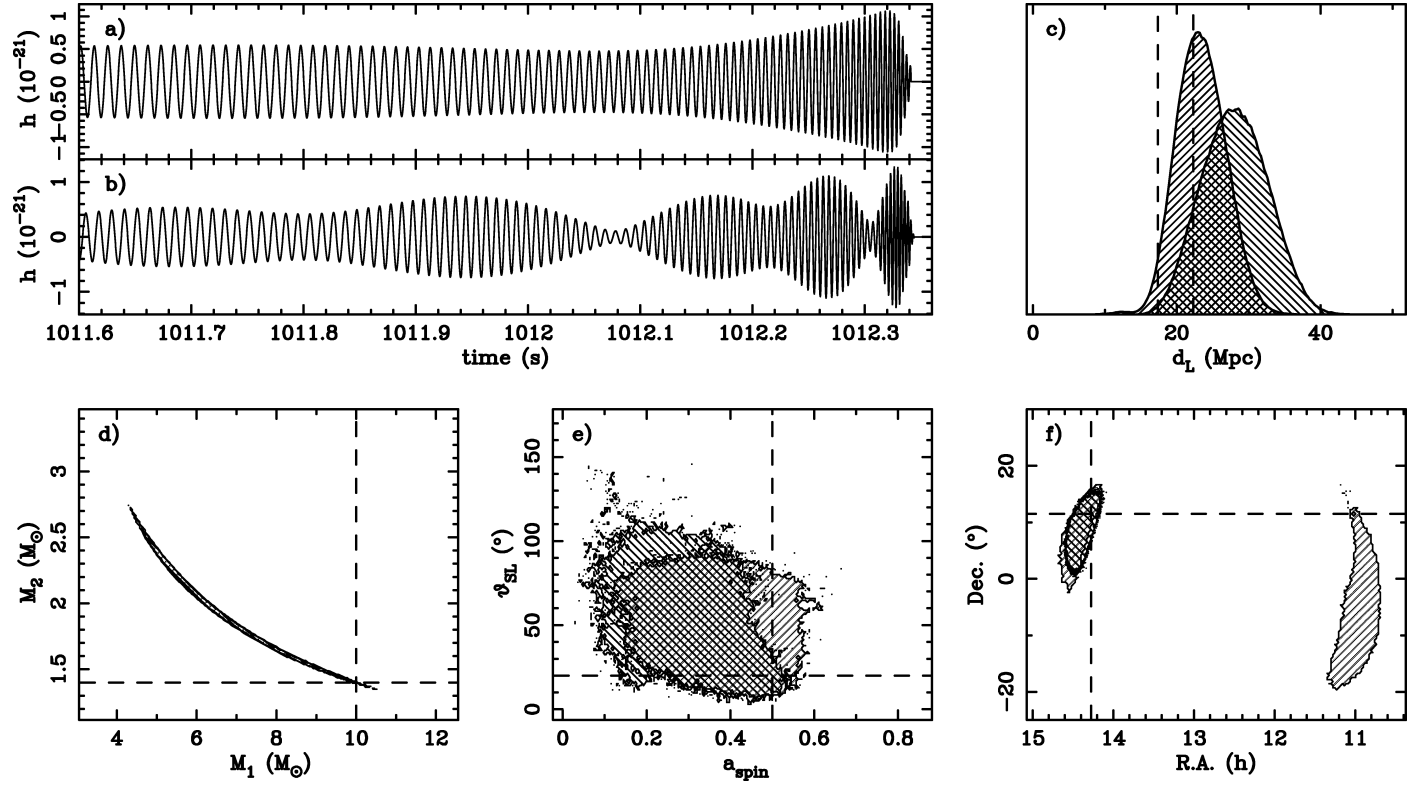


FIG. 1.—(a) Part of the waveform from a source with $a_{\text{spin}} = 0.1$ and $\theta_{\text{SL}} = 20^\circ$. (b) The same waveform, but for $a_{\text{spin}} = 0.8$. (c) Posterior PDF of the luminosity distance for a signal with $a_{\text{spin}} = 0.5$ and $\theta_{\text{SL}} = 20^\circ$, as determined with the signal of two (*left PDF*) and three (*right PDF*) detectors. The dashed lines show the true distance, which is higher for the three-detector case to obtain the same S/N. (d–f) Two-dimensional posterior PDF showing the 99% probability areas for the same runs as (c), for the individual masses, where the ellipses are aligned with the line of constant \mathcal{M} (d), the spin parameters (e), and the position in the sky (f). The dashed lines display the true parameter values. Upward and downward hashes show the result for two and three detectors respectively in panels c–f.

gorithms, more accurate waveforms (e.g., Kidder 1995; Will & Wiseman 1996; Faye et al. 2006; Blanchet et al. 2006) will be necessary for the analysis of real signals.

A circular binary inspiral with one spinning compact object is described by a 12-dimensional parameter vector λ . With respect to a fixed geocentric coordinate system our choice of independent parameters is

$$\lambda = \{\mathcal{M}, \eta, \text{R.A.}, \cos \text{Decl.}, \cos \theta_{J_0}, \phi_{J_0}, \log d_L, a_{\text{spin}}, \cos \theta_{\text{SL}}, \phi_c, \alpha_c, t_c\}, \quad (1)$$

where $\mathcal{M} = (M_1 M_2)^{3/5} / (M_1 + M_2)^{1/5}$ and $\eta = M_1 M_2 / (M_1 + M_2)^2$ are the chirp mass and symmetric mass ratio, respectively; R.A. (right ascension) and Decl. (declination) identify the source position in the sky; the angles $\theta_{J_0} \in [-\frac{\pi}{2}, \frac{\pi}{2}]$ and $\phi_{J_0} \in [0, 2\pi]$ identify the unit vector \hat{J}_0 ; d_L is the luminosity distance to the source and $0 \leq a_{\text{spin}} \equiv S/M_1^2 \leq 1$ is the dimensionless spin magnitude; ϕ_c and α_c are integration constants that specify the GW phase and the location of \mathcal{S} on the precession cone, respectively, at the time of coalescence t_c .

Given a network comprising n_{det} detectors, the data collected at the a th instrument ($a = 1, \dots, n_{\text{det}}$) is given by $x_a(t) = n_a(t) + h_a(t; \lambda)$, where $h_a(t; \lambda) = F_{a,+}(t)h_{a,+}(t; \lambda) + F_{a,\times}(t)h_{a,\times}(t; \lambda)$ is the GW strain at the detector (see eqs. [2]–[5] in Apostolatos et al. 1994) and $n_a(t)$ is the detector noise. The astrophysical signal is given by the linear combination of the two independent polarizations $h_{a,+}(t; \lambda)$ and $h_{a,\times}(t; \lambda)$ weighted by the *time-dependent* antenna beam patterns $F_{a,+}(t)$ and $F_{a,\times}(t)$. An example of h_a for $\theta_{\text{SL}} = 20^\circ$ and $a_{\text{spin}} = 0.1$ and 0.8 is shown in panels a–b of Figure 1. In our analysis we model the noise in

each detector as a zero-mean Gaussian, stationary random process, with one-sided noise spectral density $S_a(f)$ at the initial-LIGO design sensitivity, where f is the frequency.

3. PARAMETER ESTIMATION: METHODS AND RESULTS

The goal of our analysis is to determine the *posterior* PDF of the unknown parameter vector λ in equation (1), given the data sets x_a collected by a network of n_{det} detectors and the *prior* $p(\lambda)$ on the parameters. We use wide, flat priors (see Van der Sluys et al. 2008 for details). Bayes’ theorem provides a rigorous mathematical rule to assign such a probability:

$$p(\lambda|x_a) = \frac{p(\lambda)\mathcal{L}(x_a|\lambda)}{p(x_a)}; \quad (2)$$

here

$$\mathcal{L}(x_a|\lambda) \propto \exp \left[-2 \int_{f_1}^{f_h} \frac{|\tilde{x}_a(f) - \tilde{h}_a(f; \lambda)|^2}{S_a(f)} df \right] \quad (3)$$

is the *likelihood function* of the data given the model, which measures the fit of the data to the model, and $p(x_a)$ is the *marginal likelihood* or *evidence*; $\tilde{x}(f)$ stands for the Fourier component of $x(t)$. For multidetector observations involving a network of detectors with uncorrelated noise—this is the case of this Letter, where we do not use the 2 km detector at Hanford—we have $\mathcal{L}(\{x_a; a = 1, \dots, n_{\text{det}}|\lambda\}) = \prod_{a=1}^{n_{\text{det}}} \mathcal{L}(x_a|\lambda)$.

The numerical computation of the joint and *marginalized* PDFs involves the evaluation of integrals over a large number

TABLE 1
INJECTION DETAILS AND WIDTHS OF THE 90% PROBABILITY INTERVALS OF THE MCMC RUNS FOR H1 AND V, S/N = 17

n_{det}	a_{spin}	θ_{SL} (deg)	d_L (Mpc)	M_1 (%)	M_2 (%)	\mathcal{M} (%)	η (%)	t_c (ms)	d_L (%)	a_{spin}	θ_{SL} (deg)	ϕ_c (deg)	α_c (deg)	Pos. (deg ²)	Ori. (deg ²)
2	0.0	0	16.0	95	83	2.6	138	18	86	0.63	...	323	...	537	19095
	0.1	20	16.4	102	85	1.2	90	10	91	0.91	169	324	326 ^a	406	16653
	0.1	55	16.7	51	38	0.88	59	7.9	58	0.32	115	322	326	212	3749
	0.5	20	17.4	53 ^b	42 ^a	0.90	50 ^b	5.4	46 ^a	0.26	56	330	301 ^b	111 ^a	3467 ^a
	0.5	55	17.3	31	24	0.62	41	4.9	21	0.12	24	323	269 ^a	19.8	178 ^a
	0.8	20	17.9	54 ^a	42 ^a	0.86 ^a	54 ^a	6.0	56	0.16	25 ^a	325	319	104 ^a	1540
	0.8	55	17.9	21	16	0.66	29	4.7	22	0.15	15	320	323	22.8	182 ^a
3	0.0	0	20.5	114	90	2.6	119	15	69	0.98 ^b	...	325	...	116	4827
	0.1	20	21.1	70	57	0.92	72	7.0	60	0.49	160	321	322 ^a	64.7	3917
	0.1	55	21.4	62	48	0.93	68	6.2	51	0.52	123	325	308 ^a	48.7	976
	0.5	20	22.3	54 ^b	44 ^a	0.89 ^a	48 ^b	3.3	52	0.28 ^a	69	318	229 ^b	28.8	849
	0.5	55	22.0	33	25	0.62	43	4.6	23 ^a	0.14	27	322	324	20.7	234 ^a
	0.8	20	23.0	53 ^b	41 ^a	0.85 ^a	52 ^b	3.8	55	0.17	23 ^a	320	327 ^a	36.4 ^a	645
	0.8	55	22.4	30	22	0.86	40	5.0	26	0.21	21	322	323	27.2	288

^a The true value lies outside the 90% probability range.

^b The true value lies outside the 99% probability range, but inside the 100% range.

of dimensions. MCMC methods (e.g., Gilks et al. 1996; Gelman et al. 1997 and references therein) have proved to be particularly effective in tackling these numerical problems. We developed an adaptive (see Figueiredo & Jain 2002; Atchadé & Rosenthal 2005) MCMC algorithm to explore the parameter space efficiently while requiring the least amount of tuning for the specific signal at hand; the code is an extension of the one developed by some of the authors to explore MCMC methods for nonspinning binaries (Röver et al. 2006, 2007) and takes advantage of techniques explored by some of us in the context of *LISA* data analysis (Stroer et al. 2007). A summary of the methods used in our MCMC code was published (Van der Sluis et al. 2008); more technical details will be provided elsewhere.

Here we present results obtained by adding a signal in simulated initial-LIGO noise and computing the posterior PDFs with MCMC techniques for a fiducial source consisting of a $10 M_{\odot}$ spinning BH and a $1.4 M_{\odot}$ nonspinning NS in a binary system with a signal-to-noise ratio (S/N) of 17.0 (obtained by scaling the distance) for the network of two or three detectors. We consider a number of cases for which we change the BH spin magnitude ($a_{\text{spin}} = 0.0, 0.1, 0.5, 0.8$) and the angle between the spin and the orbital angular momentum ($\theta_{\text{SL}} = 20^{\circ}, 55^{\circ}$); the remaining 10 parameters, including source position and binary orientation, are kept constant (R.A. = 14.3^{h} , Decl. = 12° , $\theta_{j_0} = 4^{\circ}$, and $\phi_{j_0} = 289^{\circ}$ for this study). For each of the seven ($a_{\text{spin}}, \theta_{\text{SL}}$) combinations (six for finite spin, one for zero spin), we run the analysis using the data from (1) the 4 km LIGO detector at Hanford (H1) and the Virgo detector (V) near Pisa ($n_{\text{det}} = 2$), and (2) the two LIGO 4 km detectors (H1 and L1) and the Virgo detector ($n_{\text{det}} = 3$). This results in a total of 14 signal cases explored in this study. The MCMC analysis that we carry out on each data set consists of five separate serial chains, each with a length of 3.5×10^6 iterations ($n_{\text{det}} = 2$) or 2.5×10^6 iterations ($n_{\text{det}} = 3$), sampled after a *burn-in* period (see, e.g., Gilks et al. 1996) that is determined automatically as follows: we determine the absolute maximum likelihood L_{max} that is obtained in any of the five chains, and for each chain include all the iterations *after* the chain reached a likelihood value of $L_{\text{max}} - 2$. Each chain starts at offset (i.e., non-true) parameter values. The starting values for \mathcal{M} and t_c are drawn from a Gaussian distribution centered on the true parameter value, with a standard deviation of about $0.1 M_{\odot}$ and 30 ms respectively. The other 10 parameters are drawn randomly from the allowed ranges. Multiple chains starting from offset parameters and locking on to the same values for the parameters and likelihood provide

convincing evidence of convergence in a blind analysis. Our MCMC code needs to run for typically one week to show the first results and 10–14 days to accumulate a sufficient number of iterations for good statistics, each serial chain using a single 2.8 GHz CPU. An example of the PDFs obtained for a signal characterized by $a_{\text{spin}} = 0.5$ and $\theta_{\text{SL}} = 20^{\circ}$ is shown in panels *c–f* of Figure 1, for the cases of two and three detectors; the PDFs for M_1 and M_2 in Figure 1*d* are constructed from those obtained for \mathcal{M} and η .

To evaluate the parameter-estimation accuracy we compute probability intervals; Table 1 shows the 90% probability interval for each of the parameters, defined as the smallest range for which the posterior probability of a given parameter to be in that range is 0.9. For the two-dimensional cases (position and orientation) we quote the smallest *area* that contains 90% of the probability. Of the 140 marginalized PDFs considered here (ignoring the derived parameters M_1 , M_2 and combining R.A., Decl. as position and θ_{j_0} , ϕ_{j_0} as orientation), the true parameter values lie outside the 90% probability range in 27 cases: 21 cases are within the 99% probability range (marked with “a” in Table 1), and six cases lie outside the 99% but inside the 100% range (marked with “b” in the table).

Most of these outliers are caused by a degeneracy between the mass and spin parameters. A parameter set with different values for \mathcal{M} , η , a_{spin} , and θ_{SL} can produce a waveform that is almost identical to the signal we injected. For the chirp mass and spin parameters, the distance between the two degenerate regions is relatively small. However, for the mass ratio η , these two regions ($\eta \approx 0.11$, the injected value and $\eta \approx 0.2$) are far apart and seem disconnected. A comparison of waveforms from the two degenerate regions demonstrates that their overlap is so high (match $> 99.5\%$) that it would be impossible to tell which is the true signal even at high S/N. This degeneracy could be physical or could be caused by the simplified waveform model; further investigation is warranted.

For a detection with two interferometers, the sky position and binary orientation are degenerate; for low spin, our PDFs show an incomplete ring in the sky where the source might be. When the BH spin increases, the allowed sky location shrinks appreciably until mere arcs are left (Fig. 1*f*). For intermediate and high spin, and $\theta_{\text{SL}} = 55^{\circ}$, we typically find only one such arc, reducing the sky position to several tens of square degrees (Table 1). Thus, with two detectors the parameters can be measured at astrophysically interesting levels when suffi-

cient spin is present, including distance, individual masses, spin magnitude and tilt angle; for $a_{\text{spin}} = 0.5$ or more, the typical uncertainty in the sky position is of the order of tens of square degrees, the distance is determined with 20%–60% accuracy and the timing accuracy is 6 ms or better.

The accuracy of the parameter determination is affected by the number of detectors used, a result well established in studies of inspirals without spinning components (e.g., Jaranowski & Krolak 1994; Pai et al. 2001; Cavalier et al. 2006; Röver et al. 2007). Unlike some other studies, we keep the S/N of the detector network constant; when a third detector is added, the source distance is increased (Fig. 1c). Thus, we see the effect of the additional information that is provided by the extra detector and eliminate that of the higher S/N. Table 1 shows that the effect on the uncertainty in the mass and spin parameters is marginal when adding a third interferometer to the network. The uncertainty in the distance and time of coalescence decreases typically by 20%–25% when using three detectors, but the largest effect is on the accuracy for sky position and binary orientation; Table 1 shows that the (two-dimensional) uncertainties in the latter two quantities decrease by 50% and 40% respectively on average.

The parameter-estimation accuracy also depends strongly on the actual spin parameters of the system: the larger a_{spin} and θ_{SL} , the stronger the modulations in the waveform induced by precession, and the more information is coded up in the waveform. When we divide our simulations into low spin ($a_{\text{spin}} = 0.0, 0.1$) and high spin ($a_{\text{spin}} = 0.5, 0.8$) cases, we find that the uncertainties in the high-spin case are smaller by 40%–60% for the masses, time of coalescence and distance, by 65%–70% for the spin parameters and by 80%–90% for the sky position and binary orientation. However, the width of the 90% probability interval is in fact not strictly monotonic as a function of a_{spin} and θ_{SL} (Table 1). The increasingly complex structure of the likelihood function and stronger correlations among different parameters for higher spin have an important effect on the sampling efficiency of the MCMC.

Earlier studies (e.g., Cutler & Flanagan 1994, their Tables II and III and Fig. 7; Jaranowski & Krolak 1994; Poisson & Will 1995, their Table II; Van den Broeck & Sengupta 2007, their Table III) reported on the theoretical accuracy of parameter estimation. These explorations are based on the Fisher matrix, which yields the expected uncertainty (for unimodal distributions), without actually estimating the parameter values themselves. They focus on objects with zero or (anti)aligned spin, whereas we consider precessing systems. The quoted accuracies

for masses and the time and phase of coalescence are typically better than or similar to the values in our Table 1. We were able to estimate distance, sky position and binary orientation to better accuracy than suggested in these studies.

4. CONCLUSIONS

We explored for the first time the parameter estimation of all physical parameters—including masses, spin, distance, sky location and binary orientation—on ground-based gravitational-wave observations of binary inspirals with spinning compact objects. We show that for two detectors and sufficient spin ($a_{\text{spin}} \geq 0.5$) or for three detectors, the obtained accuracy in sky position, distance and time of coalescence is good enough to allow the identification of electromagnetic counterparts of compact-binary mergers, e.g., short gamma-ray bursts (Nakar 2007). A direct measurement of mass, spin, distance and orientation can be obtained from inspiral GWs, which is notoriously difficult for electromagnetic observations.

The analysis presented here is the first step of a more detailed study that we are currently carrying out, exploring a much larger parameter space, developing techniques to reduce the computational cost of these simulations, and testing the methods with actual LIGO data. The waveform model used here, although adequate for exploratory studies, is not sufficiently accurate for the analysis of real detections, and we are finalizing the implementation of a more realistic waveform. Simulations with this improved waveform may also shed light on the degeneracy between mass and spin parameters discussed in § 3, and may improve the accuracy of our parameter estimation appreciably (e.g., Van den Broeck & Sengupta 2007). Finally, we intend to further develop our Bayesian approach into a standard tool that can be included in the analysis pipeline used for the processing of the “science data” collected by ground-based laser interferometers.

This work is partially supported by a Packard Foundation Fellowship, a NASA BEFS grant (NNG06GH87G), and a NSF Gravitational Physics grant (PHY-0353111) to V. K.; NSF Gravitational Physics grant PHY-0553422 to N. C.; Royal Society of New Zealand Marsden Fund grant UOA-204 to R. M. and C. R.; and UK Science and Technology Facilities Council grant to A. V. Computations were performed on the Fugu computer cluster funded by NSF MRI grant PHY-0619274 to V. K.

REFERENCES

- Acernese, F., et al. 2004, *Classical Quantum Gravity*, 21, S385
 Apostolatos, T. A., Cutler, C., Sussman, G. J., & Thorne, K. S. 1994, *Phys. Rev. D*, 49, 6274
 Atchadé, Y. F., & Rosenthal, J. S. 2005, *Bernoulli*, 11, 815
 Barish, B. C., & Weiss, R. 1999, *Phys. Today*, 52, 44
 Blanchet, L., Buonanno, A., & Faye, G. 2006, *Phys. Rev. D*, 74, 104034
 Buonanno, A., Chen, Y., & Vallisneri, M. 2003, *Phys. Rev. D*, 67, 104025
 Cavalier, F., et al. 2006, *Phys. Rev. D*, 74, 082004
 Cutler, C., & Flanagan, E. E. 1994, *Phys. Rev. D*, 49, 2658
 Cutler, C., & Thorne, K. S. 2002, preprint (gr-qc/0204090)
 Faye, G., Blanchet, L., & Buonanno, A. 2006, *Phys. Rev. D*, 74, 104033
 Figueiredo, M. A. T., & Jain, A. K. 2002, *IEEE Trans. Pattern Analysis and Machine Intelligence*, 24, 381
 Gelman, A., Carlin, J. B., Stern, H., & Rubin, D. B. 1997, *Bayesian Data Analysis* (Boca Raton: Chapman & Hall)
 Gilks, W. R., Richardson, S., & Spiegelhalter, D. J. 1996, *Markov Chain Monte Carlo in Practice* (London: Chapman & Hall/CRC)
 Grandclément, P., Kalogera, V., & Vecchio, A. 2003, *Phys. Rev. D*, 67, 042003
 Jaranowski, P., & Krolak, A. 1994, *Phys. Rev. D*, 49, 1723
 Kidder, L. E. 1995, *Phys. Rev. D*, 52, 821
 Lang, R. N., & Hughes, S. A. 2006, *Phys. Rev. D*, 74, 122001
 Nakar, E. 2007, *Phys. Rep.*, 442, 166
 O’Shaughnessy, R., Kim, C., Kalogera, V., & Belczynski, K. 2008, *ApJ*, 672, 479
 Pai, A., Dhurandhar, S., & Bose, S. 2001, *Phys. Rev. D*, 64, 042004
 Poisson, E., & Will, C. M. 1995, *Phys. Rev. D*, 52, 848
 Röver, C., Meyer, R., & Christensen, N. 2006, *Classical Quantum Gravity*, 23, 4895
 ———. 2007, *Phys. Rev. D*, 75, 062004
 Stroeer, A., et al. 2007, *Classical Quantum Gravity*, 24, 541
 Van den Broeck, C., & Sengupta, A. S. 2007, *Classical Quantum Gravity*, 24, 1089
 Van der Sluys, M., Raymond, V., Mandel, I., Röver, C., Christensen, N., Kalogera, V., Meyer, R., & Vecchio, A. 2008, *Classical Quantum Gravity*, 25, 184011
 Vecchio, A. 2004, *Phys. Rev. D*, 70, 042001
 Will, C. M., & Wiseman, A. G. 1996, *Phys. Rev. D*, 54, 4813
 Willke, B., et al. 2004, *Classical Quantum Gravity*, 21, 417